COSMIC AND SUBATOMIC PHYSICS REPORT
LUIP 9902
FEBRUARY 1999
ISRN LUNFD6/NFFK-7161-SE+14P
ISSN 0348-9329

Investigating pre-equilibrium and equilibrium neutron emission in the 45 MeV/nucleon ^{58}Ni + ^{27}Al reaction via two-neutron interferometry

R. Ghetti[a,b], N. Colonna[a], E. De Filippo[c,d], J. Helgesson[e], G. Tagliente[a], A. Anzalone[f], V. Bellini[d,f], L. Carlèn[b], S. Cavallaro[d,f], L. Celano[a], G. D'Erasmo[a], D. Di Santo[a], E.M. Fiore[a], A. Fokin[b], M. Geraci[c], B. Jakobsson[b], A. Kuznetsov[g], G. Lanzanó[c,d], D. Mahboub[f], Yu. Murin[b], J. Mårtensson[b], A. Pagano[c,d], F. Palazzolo[f], M. Palomba[a], A. Pantaleo[a], V. Paticchio[a], R. Potenza[d], G. Riera[f], A. Siwek[b], M.L. Sperduto[d,f], C. Sutera[c,d], M. Urrata[f], L. Westerberg[h]

(CHIC Collaboration)

[a] *Istituto Nazionale Fisica Nucleare and Dip. di Fisica, V. Amendola 173, I-70126 Bari, Italy*

[b] *Department of Physics, Lund University, Box 118, SE-221 00 Lund, Sweden*

[c] *Istituto Nazionale Fisica Nucleare, Sezione di Catania, Corso Italia 57, I-95129 Catania, Italy*

[d] *Dipartimento di Fisica, Universitá di Catania, Corso Italia 57, I-95129 Catania, Italy*

[e] *School of Engineering and Economics, Malmö University, SE-205 06 Malmö, Sweden*

[f] *Istituto Nazionale Fisica Nucleare, Laboratori Nazionali del Sud, Via S. Sofia 44, I-95123 Catania, Italy*

[g] *Khlopin Radium Inst., St. Petersburg, Russia*

[h] *The Svedberg Laboratory, Uppsala, Sweden*

Cosmic and Subatomic Physics
University of Lund
Sölvegatan 14
S-223 62 Lund, Sweden

CERN LIBRARIES, GENEVA
SCAN-9911048

Investigating pre-equilibrium and equilibrium neutron emission in the 45 MeV/nucleon ^{58}Ni + ^{27}Al reaction via two-neutron interferometry

R. Ghetti[a,b], N. Colonna[a], E. De Filippo[c,d], J. Helgesson[e], G. Tagliente[a], A. Anzalone[f], V. Bellini[d,f], L. Carlèn[b], S. Cavallaro[d,f], L. Celano[a], G. D'Erasmo[a], D. Di Santo[a], E.M. Fiore[a], A. Fokin[b], M. Geraci[c], B. Jakobsson[b], A. Kuznetsov[g], G. Lanzanó[c,d], D. Mahboub[f], Yu. Murin[b], J. Mårtensson[b], A. Pagano[c,d], F. Palazzolo[f], M. Palomba[a], A. Pantaleo[a], V. Paticchio[a], R. Potenza[d], G. Riera[f], A. Siwek[b], M.L. Sperduto[d,f], C. Sutera[c,d], M. Urrata[f], L. Westerberg[h]

(CHIC Collaboration)

[a] *Istituto Nazionale Fisica Nucleare and Dip. di Fisica, V. Amendola 173, I-70126 Bari, Italy*

[b] *Department of Physics, Lund University, Box 118, SE-221 00 Lund, Sweden*

[c] *Istituto Nazionale Fisica Nucleare, Sezione di Catania, Corso Italia 57, I-95129 Catania, Italy*

[d] *Dipartimento di Fisica, Universitá di Catania, Corso Italia 57, I-95129 Catania, Italy*

[e] *School of Engineering and Economics, Malmö University, SE-205 06 Malmö, Sweden*

[f] *Istituto Nazionale Fisica Nucleare, Laboratori Nazionali del Sud, Via S. Sofia 44, I-95123 Catania, Italy*

[g] *Khlopin Radium Inst., St. Petersburg, Russia*

[h] *The Svedberg Laboratory, Uppsala, Sweden*

(November 23, 1998)

Abstract

In this paper we present the two-neutron correlation function measured from the ^{58}Ni + ^{27}Al reaction at 45 MeV/nucleon. A comparison to BUU and evaporation calculations indicates that the bulk of neutron emission is explained by the evaporative process. However, one component, selected with the cri-

terion of a high total momentum of the particle pair, is not accounted for by evaporation. This component can be identified as pre-equilibrium emission.

Two-particle interferometry has become a widely used technique to probe the dynamical evolution of nuclear collisions [1]. In particular, two-neutron correlation functions constitute a powerful tool to study the space-time extent of excited nuclear systems. The parameters characterizing neutron emission are not distorted by the Coulomb interaction and can be deduced from the interplay of quantum statistical and nuclear interaction effects alone.

In intermediate energy heavy ion collisions, two-nucleon interferometry may be used to study the interplay between dynamical and statistical effects in particle emission, in particular to disentangle the contribution of the early pre-equilibrium emission [2] from the slower deexcitation processes [3]. The spectral shape and the time scale of pre-equilibrium emission, often known only in a model-dependent way, may be probed experimentally with two-neutron correlation functions, by applying a selection on large momentum nucleons [4].

In this paper we report on a study of two-neutron interferometry in the intermediate energy regime. The experiment was performed with an E/A = 45 MeV ^{58}Ni beam impinging on a $\sim$ 5 mg/cm^2 thick Al target foil [5]. The beam was provided by the Superconducting Cyclotron of Laboratori Nazionali del Sud, Catania, Italy.

The neutron device consisted of 48 BC501A liquid scintillator cylindrical cells, 12.7 cm in diameter by 12.7 cm thickness [6]. The neutron detectors were mounted in 4 clusters placed at 2.7 m from the target in the horizontal plane, at angular positions of 90° and 45° on one side of the beam, and 45° and 25° on the other side. Each cluster consisted of 12 detectors arranged in a matrix of 5x5 cells, with two consecutive detectors separated by an empty cell. A minimum separation of $\sim$ 4.5° between adjacent detectors was achieved in this way. For a particular cross-talk investigation, two detectors in one of the 45° clusters were radially shifted backwards, to a distance of 3.4 m from the target. For event selection, a forward wall for fragment detection was set up [7,8]. The wall, consisting of 36 phoswich BaF_2 scintillators, was positioned 2 m from the target and covered angles between 1 and 8°.

The neutron energy was determined from the time of flight measurement between the

cyclotron RF signal and the liquid scintillator signal. The total time resolution measured from the width of the prompt γ-ray peak was $\sim$ 2 ns. Due to a burst suppression system, a 118 ns time window between beam bursts could be achieved and this allowed registration of neutrons down to 2.3 MeV. A relative momentum threshold of $\sim$ 3 MeV/c was therefore achieved in the measurement.

The neutron data were sorted with a first requirement that at least one fragment should be detected in the forward wall and that two neutron detectors should be fired. After performing n/γ discrimination, the data sample was reduced to two-neutron coincidence events and neutron singles (from neutrons originally detected in coincidence with one γ-ray).

Two-neutron coincidence events are affected by a large background contamination due to cross-talk between neighboring detectors (i.e. the interaction and registration of the same neutron in two different detectors). Event-by-event Monte Carlo simulations, performed with a revised version of the computer code MENATE [9] and a software replica of the experimental apparatus, predict a cross-talk event yield of $\sim$ 30 - 40 % of the total coincidence yield. This value agrees with the result of an empirical method devised to grossly estimate the cross-talk probability from the experimental coincidence data sample.

In order to generate cross-talk-free correlation functions from which reliable conclusions on the space-time extent of the emitting source can be extracted, the raw data have to be corrected for these spurious cross-talk coincidences by applying a cross-talk rejection procedure [10–13]. The procedure used in the present data analysis is the one investigated for an equidistant detector configuration (see refs. [11,14]). With such a configuration, a genuine coincidence can be identified by requiring that the second neutron does not satisfy the kinematic constraints imposed by the scattering. A false coincidence can be rejected by requiring that the following condition is fulfilled:

$$E_1 > E_{min} = \frac{1}{2} m \frac{d_{min}^2}{\Delta t^2}. \qquad (1)$$

Here, E_1 is the energy of the first neutron. E_{min} is the minimum energy required by the

neutron scattered from the first detector to travel the minimum distance d_{min} to the second detector, in the time interval $\Delta t = t_2 - t_1$. For a cross-talk event, E_{min} is less or equal to the energy of the scattered neutron.

The event-by-event Monte Carlo simulations mentioned above, indicate that all cross-talk events are rejected by condition (1) along with a large number of true coincidences. As shown in ref. [14], however, the loss of true coincidences does not introduce a noticeable bias, as long as the denominator is properly constructed (i.e. the rejection condition applied to the correlated sample is applied also to the uncorrelated yield).

The experimental setup allowed us to check also a different cross-talk rejection procedure. Since two of the neutron detectors were shifted backwards we could perform the nn analysis for neutron detector pairs with different distances from the target and apply the cross-talk rejection procedure suggested in ref. [13]. The results from this analysis were found in good agreement with those from the "equidistant" detector configuration.

The correlation function was constructed as:

$$C(q) = K \cdot \frac{N_{12}(p_1 p_2)}{N_1(p_1) N_2(p_2)} \tag{2}$$

i.e. by dividing the coincidence yield by the yield for uncorrelated events and normalizing with a constant, determined so that $C(q)$ approaches unity at large values of q (> 30 MeV/c). The denominator was constructed from the product of single distributions since one-particle observables are not affected by cross-talk [15] and the background spectrum of relative momenta is unbiased. Compensation for the true coincidences rejected in the numerator (therefore affecting the neutron energy distribution) was performed by applying the cross-talk rejection to the uncorrelated pairs.

The solid line in fig. 1 represents the experimental inclusive neutron kinetic energy spectrum in the laboratory frame. The distribution exhibits the expected Boltzmann-like shape shifted with the source velocity in the laboratory frame.

The two-neutron correlation function obtained from equidistant detector pairs in coincidence with at least one hit in the forward wall, is shown by the solid dots in fig. 2.

In order to interpret the experimental results, we have confronted both the correlation function and the single particle data with the predictions from two complementary and well established theoretical models.

The evaporation model of ref. [16] describes the ensemble averaged evolution of an excited system that statistically emits particles. It assumes a time dependent evaporative emission of particles from an excited source and predicts the position, time and energy of the emitted particles. The source is specified by the initial mass and charge, excitation energy and level density parameter [17]. The advantage of this model is that it is characterized by a few global parameters, while its disadvantage is the lack of pre-equilibrium emission and impact parameter averaging.

The semi-classical Boltzmann-Uehling-Uhlenbeck (BUU) model, on the other hand, is a dynamical transport model that accounts for pre-equilibrium emission. In the version of ref. [18] the two colliding nuclei are initially in their ground states. The phase-space distribution of the source function is discretized by introducing a number of "test-particles" per nucleon that propagate in a density dependent mean field. In addition, nucleon-nucleon collisions with Pauli blocking are included.

The theoretical correlation function was obtained by convoluting the phase-space distribution, generated with either one of the above source models, with the two-neutron relative wave function calculated in the framework of the Koonin-Pratt formalism [19,20]. For each neutron pair emitted from the source, a weight was calculated, taking into account antisymmetrization and final state interactions of the neutrons. The correlation function was then constructed by summing over all pairs.

All theoretical calculations were filtered to account for the experimental energy thresholds, the energy and position resolution and all experimental efficiencies. Furthermore, all background corrections (in particular the cross-talk rejection) were incorporated into the calculations in exactly the same fashion as in the data analysis [14].

The results indicated by the star symbols in fig. 1 and by the dashed line in fig. 2 were obtained from an evaporative calculation performed under the assumption that complete

fusion takes place initially, without any loss of thermal energy due to compression or any loss of nucleons due to non-thermal pre-equilibrium processes. The evaporative source was described by mass and charge: A = 85, Z = 41 (i.e. the size of the total system) and initial excitation energy E^* = 10 MeV/nucleon (corresponding to the maximum energy in the total fusion limit). The level density parameter was fixed at a = A/15 and a center of mass velocity v_{source} = 0.2 c was added to perform a transformation into the laboratory frame.

Fig. 1 shows that the predicted kinetic energy spectrum (star symbols) compares quite well with the experimental one. The corresponding correlation function (dashed line in fig. 2), shows however a larger strength than the experimental one. Note that, even though the evaporative model contains no a priori pre-equilibrium emission, by using all available energy as excitation energy the evaporation occurs on a sufficiently fast time scale which might "simulate" some of the pre-equilibrium emission.

One reason for the overprediction of the correlation function could be the assumption of a completely fused system simulating only central collisions. Since no impact parameter selection has been performed, the experimental data contain contributions also from peripheral collisions. To illustrate this in the simplest possible way, we also performed an evaporative calculation with two sources representing a b = 6 fm collision. The parameters for the two sources were chosen as: A_T = 27, Z_T = 13, E^*_T = 2 MeV/nucleon, $v_{T source}$ = 0.06 c; A_P = 58, Z_P= 28, E^*_P = 2 MeV/nucleon, $v_{P source}$ = 0.27 c. As seen in fig. 2 (dotted line), the correlation is now in closer agreement with the experimental results (except for the two lowest relative momentum points), but the agreement of the energy spectrum (fig. 1, triangles) is somewhat worse.

The BUU calculations, on the other hand, were obtained by geometrical averaging over the range of impact parameters b = 1 - 8 fm. The simulations were performed with 500 test particles per nucleon, a density cutoff value of 0.01330 fm^{-3} to define "free" nucleons and a cutoff time of 200 fm/c to stop the calculations. A Skyrme parameterization of the nuclear potential was used and the mean field was calculated as: $U = -124(\rho/\rho_0) + 65(\rho/\rho_0)^2 + U_{Coloumb}$ (MeV).

In figs. 1 and 2 it is seen that the BUU kinetic energy spectrum shows too high "temperature" (slope parameter) and that the correlation function gives a too strong correlation in comparison with the experimental data. These results are not unexpected since the BUU model describes well the initial stage of the collision, but, since the evolution is stopped at t = 200 fm/c, it does not contain the late evaporation from equilibrium sources.

In order to isolate the contribution of the pre-equilibrium component in the data, a momentum-gated correlation function has been constructed. The gates were applied to the total momentum of the neutron pairs calculated in the reference frame of the source [21]. Fig. 3 shows the increase in the correlation function strength observed when only pairs with total momentum larger than 270 MeV/c are selected. This enhancement reflects a smaller space-time extent of the emission source.

One can notice that the high momentum pairs, representing $\sim$ 15 % of the total cross-talk rejected yield, generate a correlation function that compares well with the BUU results. This indicates their origin from the early stages of the deexcitation process where the neutron density should be high.

In summary, the experimental neutron energy distribution and the two-neutron correlation function have been compared with the predictions from an evaporative model and from the BUU transport model. We find that the results of these two complementary models are consistent with the picture of a pre-equilibrium component emitted on a fast time scale, followed by evaporative emission.

A hybrid model with contributions from both evaporative and BUU models, will be natural to use when a more refined selection of impact parameters from the BaF_2 wall information has been performed.

The authors wish to thank G. Iacobelli, M. Sacchetti, P. Vasta, A. Masciullo, G. Poli, F. Giustolisi, N. Guardone, V. Sparti for technical support and the LNS accelerator crew for providing a high quality pulsed beam. Financial support from "Knut och Alice Wallenberg" and from "Helmuth Hertz" Foundations is gratefully acknowledged by RG. The support from the Swedish Natural Science Research Council is appreciated.

Figure Captions

FIG. 1. Comparison of experimental (solid line) and theoretical (symbols) neutron kinetic energy spectra in the laboratory frame. The energy distributions $f(E)$ are arbitrarily rescaled so that $f(E_0) = 0.3$ for $E_0 = 45$ MeV.

FIG. 2. Comparison of the experimental nn correlation function (solid dots) with the theoretical correlation functions predicted by the evaporative model and by the BUU model.

FIG. 3. The experimental nn correlation function for high total momentum neutron pairs (open dots) is enhanced (compare with solid dots) and in good agreement with the BUU calculation (solid line).

REFERENCES

[1] D.H. Boal, C.K. Gelbke and B.K. Jennings, Rev. Modern Phys. **62** (1990) 553, and references therein.

[2] D.E. Fields, K. Kwiatkowski, D. Bonser, R.W. Viola, V.E. Viola, W.G. Lynch, J. Pochodzalla, M.B. Tsang, C.G. Gelbke, D.J. Fields, S.M. Austin, Phys. Lett. B **220** (1989) 356.

[3] S.J. Gaff, A. Galonsky, C.K. Gelbke, T. Glashmacher, M. Huang, J.J. Kruse, G.J. Kunde, R. Lemmon, W.G. Lynch, M.B. Tsang, J. Wang, P.D. Zecher, F. Deák, Á. Horváth, Á. Kiss, Z. Seres, K. Ieki, Y. Iwata, Phys. Rev. C **54** (1998) 2161.

[4] M. Cronqvist, Ö. Skeppstedt, M. Berg, L. Carlén, R. Elmér, R. Ghetti, J. Helgesson, B. Jakobsson, B. Norén, A. Oskarsson, F. Merchez,D. Rebreyend, L. Westerberg, V. Avdeichikov, A. Bogdanov, O. Lozhkin, Yu. Murin, K. Nybø, E. Olberg, T.F. Thorsteinsen, Phys. Lett. B **317** (1993) 505.

[5] N. Colonna, R. Ghetti, B. Jakobsson, E. De Filippo, G. Tagliente, V. Bellini, L. Carlén, S. Cavallaro, L. Celano, G. D'Erasmo, D. Di Santo, E.M. Fiore, A. Fokin, M. Geraci, J. Helgesson, A. Kuznetsov, G. Lanzanó, J. Mårtensson, D. Mahboub, A. Pagano, F. Palazzolo, M. Palomba, A. Pantaleo, V. Paticchio, R. Potenza, G. Riera, V. Russo, L. Sperduto, C. Sutera, M. Urrata, L. Westerberg, Proceedings of the 2nd Catania Relativistic Ion Studies (CRIS98), Acicastello, Italy, June 8-12, (1998). ECT* Report N. ECT*-98-011.

[6] N. Colonna, L. Celano, G. D'Erasmo, E.M. Fiore, L. Fiore, V. Paticchio, G. Tagliente, G. Antuofermo, G. Iacobelli, M. Sacchetti, P. Vasta, A. Pantaleo, Nucl. Instr. and Meth. A **381** (1996) 472.

[7] G. Lanzanó, A. Pagano, E. De Filippo, E. Pollacco, R. Barth, B. Berthier, E. Berthoumieux, Y. Cassagnou, Sl. Cavallaro, J.L. Charvet, A. Cunsolo, R. Dayras, A.

Foti, S. Harar, R. Legrain, V. Lips, C. Mazur, E. Norbeck, S. Urso, C. Volant, Nucl. Instr. and Meth. A **323** (1992) 694.

[8] G. Lanzanó, A. Pagano, S. Urso, E. De Filippo, B. Berthier, J.L. Charvet, R. Dayras, R. Legrain, R. Lucas, C. Mazur, E. Pollacco, J.E. Sauvestre, C. Volant, R. Beck, B. Djerraud, B. Hensch, Nucl. Instr. and Meth. A **312** (1992) 515.

[9] P. Désesquelles, A.J. Cole, A. Giorni, D. Heuer, A. Lleres, C. Morand, J. Saint-Martin, P. Stassi, J.B. Viano, B. Chambon, B. Cheynis, D. Drain, C. Pastor, Nucl. Instr. and Meth. A **307** (1991) 366.

[10] R. Gentner, K. Keller, W. Lücking, L. Lassen, Z. Phys. A **343** (1992) 401.

[11] N. Colonna, D.R. Bowman, L. Celano, G. D'Erasmo, E.M. Fiore, L. Fiore, A. Pantaleo, V. Paticchio, G. Tagliente, S. Pratt, Phys. Rev. Lett. **75** (1995) 4190.

[12] J. Wang, A. Galonsky, J.J. Kruse, P.D. Zecher, F. Deák, Á. Horváth, Á. Kiss, Z. Seres, K. Ieki, Y. Iwata, Nucl. Instr. and Meth. A **397** (1997) 380.

[13] J. Pluta, G. Bizard, P. Désesquelles, A. Długosz, O. Dorvaux, P. Duda, D. Durand, B. Erazmus, F. Hanappe, B. Jakobsson, C. Lebrun, F.R. Lecolley, R. Lednicky, P. Leszczyński, K. Mikhailov, K. Miller, B. Norén, T. Pawlak, M. Przewłocki, Ö. Skeppstedt, A. Stavinsky, L. Stuttgé, B. Tamain, K. Wosińska, Nucl. Instr. and Meth. A **411** (1998) 417.

[14] R. Ghetti, N. Colonna, J. Helgesson, Nucl. Instr. and Meth. A, in press.

[15] A.V. Kuznetsov, I.D. Alkhazov, D.N. Vakhtin, V.G. Lyapin , V.A. Rubchenya, W.H. Trzaska, K. Loberg, A.V. Daniel, Nucl. Instr. and Meth. A **346** (1994) 259.

[16] W.A. Friedman, W.G. Lynch, Phys. Rev. C **28** (1983) 16.

[17] Evaporation code implemented by S. Pratt, private communication (1993).

[18] W. Bauer, Nucl. Phys. **A471** (1987) 604.

[19] S.E. Koonin, Phys. Lett. B **70** (1977) 43.

[20] S. Pratt and M.B. Tsang, Phys. Rev. C **36** (1987) 2390.

[21] P.A. DeYoung, R. Bennink, T. Butler, W. Chung, C. Dykstra, G. Gilfoyle, J. Hinnefeld, M. Kaplan, J.J. Kolata, R.A. Kryger, J. Kugi, C. Mader, M. Nimchek, P. Santi, A. Snyder, Nucl. Phys. **A597** (1996) 127.

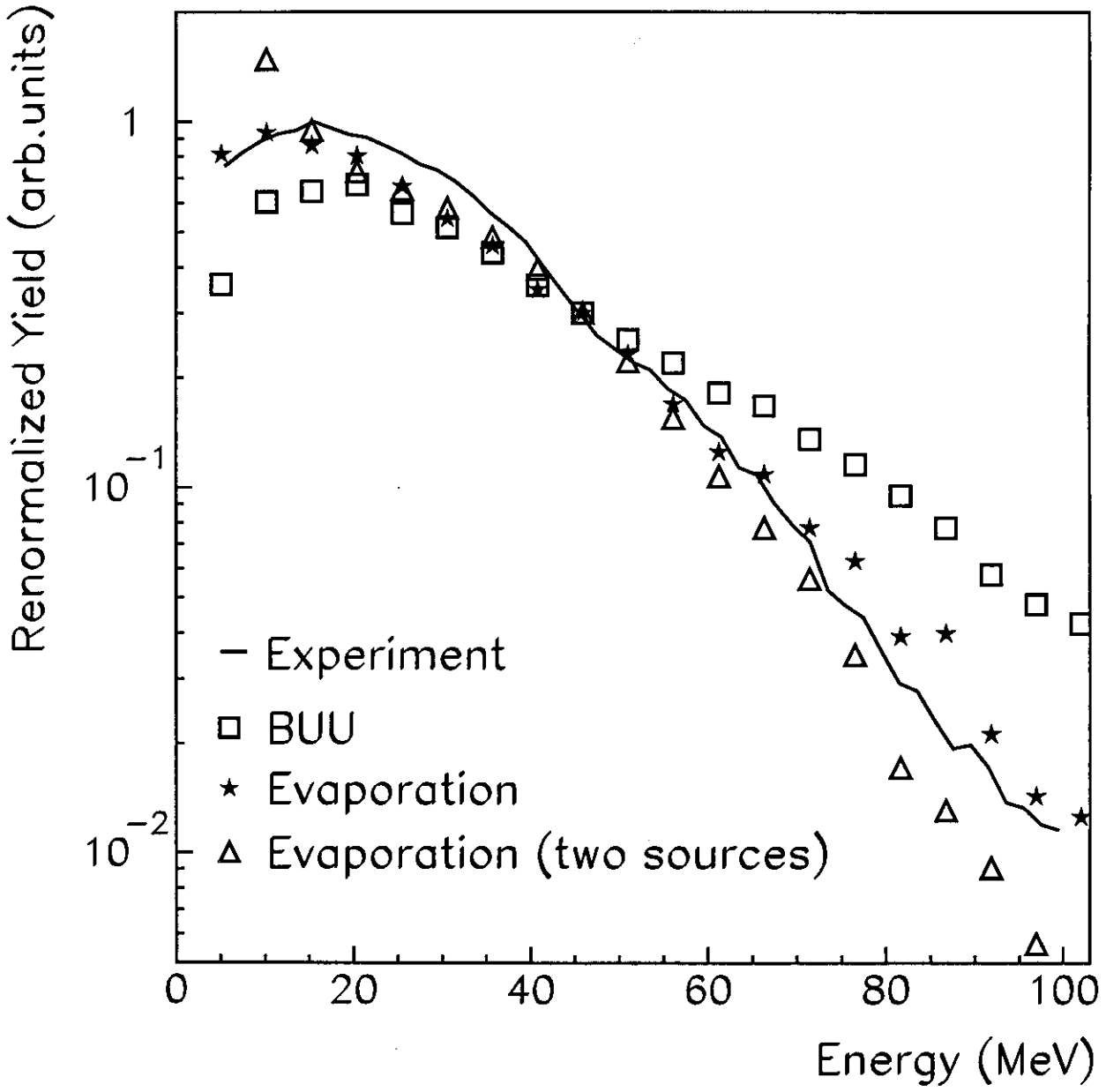
Renormalized Yield (arb.units)
1
10^{-1}
10^{-2}
0
20
40
60
80
100
Energy (MeV)
Experiment
BUU
Evaporation
Evaporation (two sources)

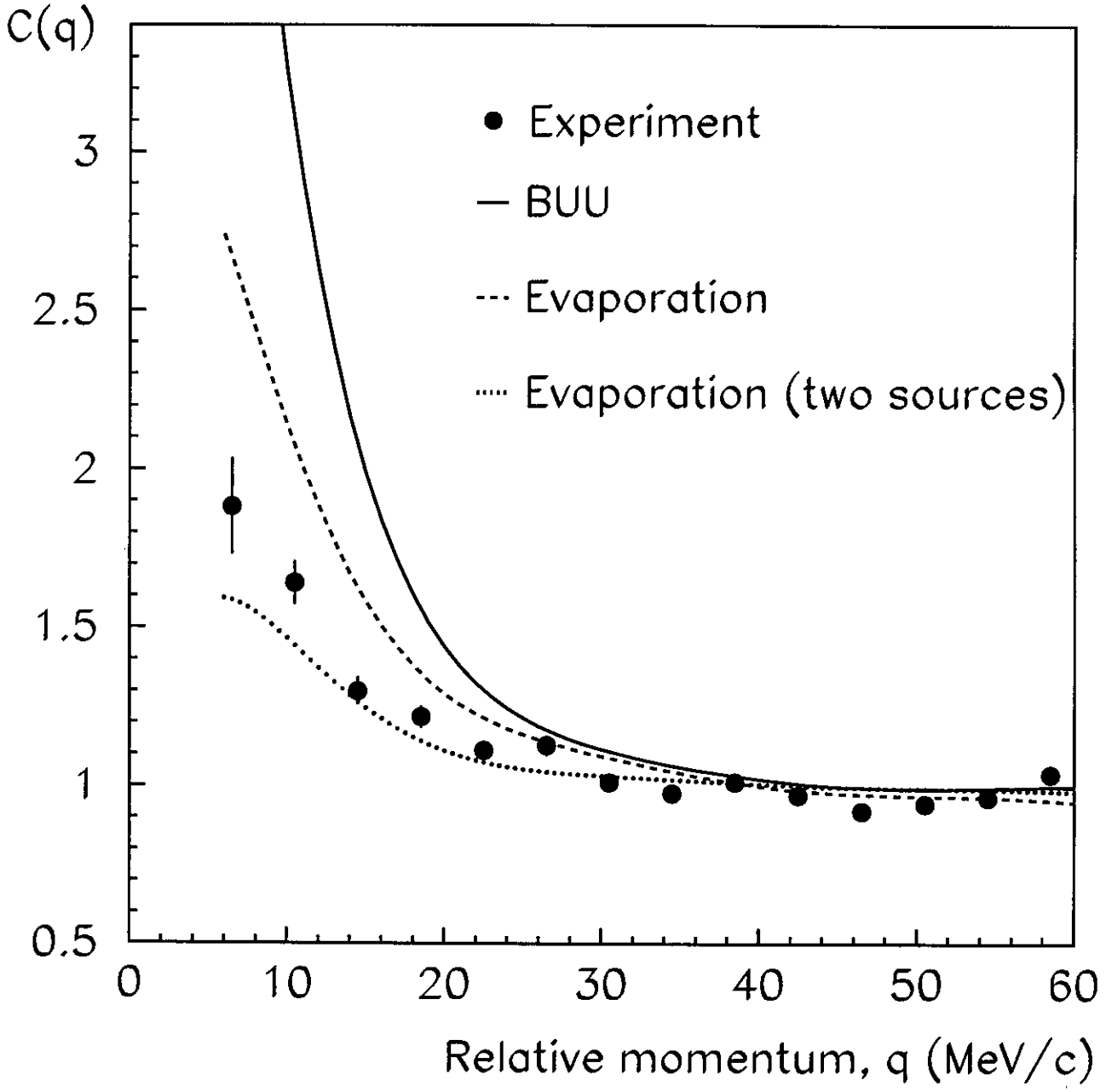
C(q)
3
2.5
2
1.5
1
0.5
0
10
20
30
40
50
60
Experiment
BUU
Evaporation
Evaporation (two sources)
Relative momentum, q (MeV/c)

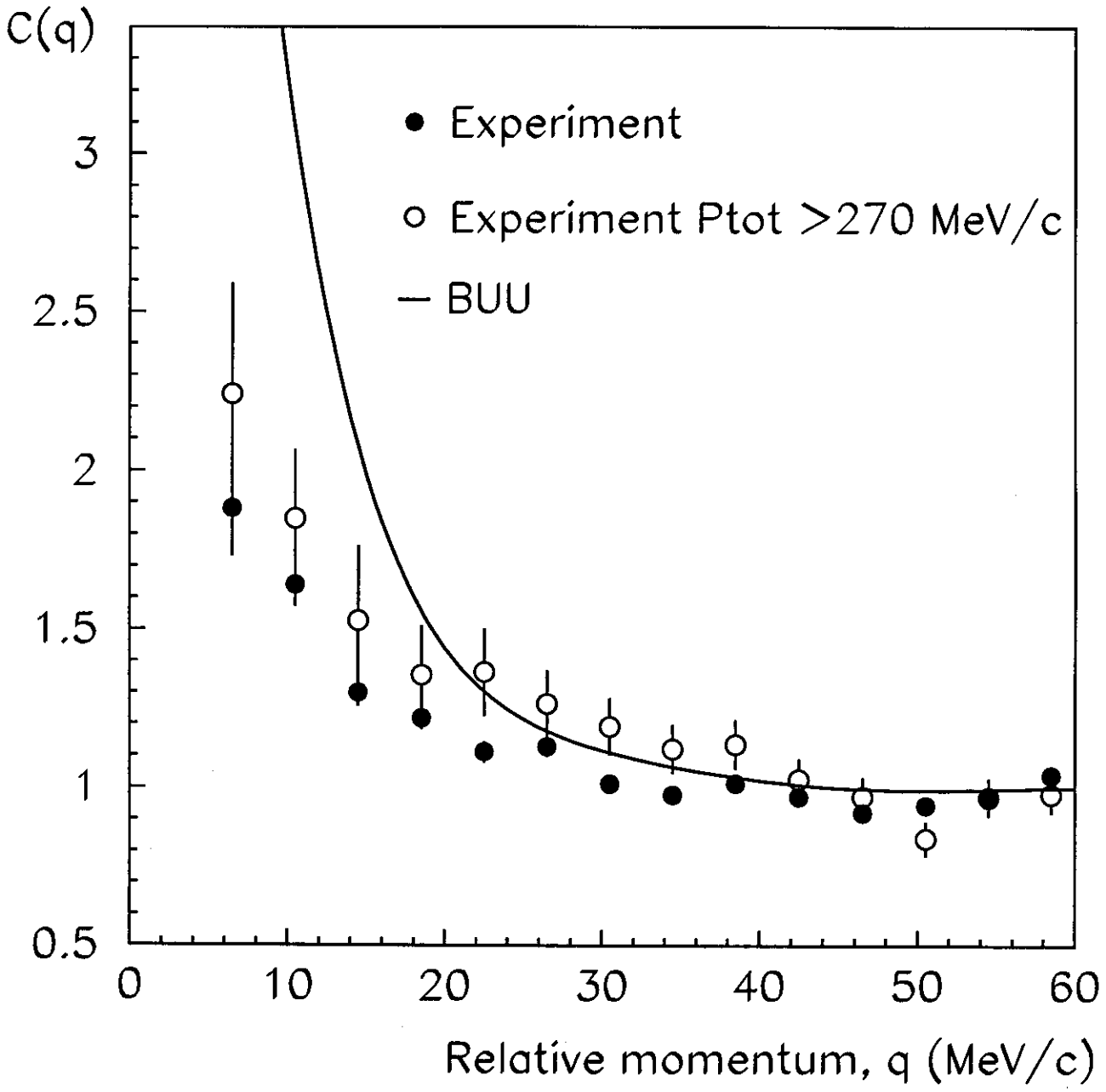
C(q)
3
2.5
2
1.5
1
0.5
0
10
20
30
40
50
60
Experiment
Experiment Ptot >270 MeV/c
BUU
Relative momentum, q (MeV/c)